Anomalous suppression of valley splittings in lead salt nanocrystals without inversion center

A. N. Poddubny,[1] M. O. Nestoklon,[1] and S. V. Goupalov[1,2]

[1]*Ioffe Physical-Technical Institute, 26 Polytekhnicheskaya Street, 194021 Saint Petersburg, Russia*

[2]*Department of Physics, Jackson State University, Jackson, Mississippi 39217, USA*

(Received 8 November 2011; revised manuscript received 1 May 2012; published 25 July 2012)

We demonstrate that confinement-induced intervalley splittings of electron energy levels in PbSe and PbS nanocrystals are sensitive to the arrangement of atoms within a nanocrystal. The splittings are strongly suppressed for stoichiometric nanocrystals of T_d point symmetry lacking a center of inversion as opposed to nonstoichiometric nanocrystals of O_h point symmetry having an inversion center. Our findings are supported by both atomistic $sp^3d^5s^*$ tight-binding calculations and a symmetry analysis.

DOI: 10.1103/PhysRevB.86.035324 PACS number(s): 73.63.Bd, 73.63.Kv

I. INTRODUCTION

Interest in almost spherical nanocrystals (NCs) made of lead chalcogenides (PbSe, PbS) has recently exploded due to their enabling potential for applications in photovoltaics.[1–5] Lead chalcogenides have band extrema in the four inequivalent L points of the Brillouin zone, and such effects as confinement-induced valley mixing and effective mass anisotropy should be considered to fully account for the properties of lead salt NCs.[6,7] Moreover, the theoretical description of lead salts on the atomistic level is challenging due to the fact that the ionicity of chemical bonds and spin-orbit interaction strength are much larger as compared to most semiconductors. As a result, many conventional approximations in the electronic structure calculations should be reconsidered when applied to lead chalcogenides.

It has been demonstrated that lead salt NCs can be synthesized by a multitude of techniques.[8] Although their crystalline structure has been experimentally established[9–11] the stoichiometry, point symmetry, and structural homogeneity of lead salt NCs grown by different procedures remain the subjects of discussions.[11–13] It is therefore important to study how the variations in NC structure affect the energies of confined electrons. In this work we consider NCs of an almost spherical shape centered on an anion or cation atom, serving as a center of inversion, along with NCs having no inversion symmetry and study how these structural variations influence the valley-orbit and spin-orbit splittings of one-particle energy levels of confined electrons and holes. We found that in NCs without a center of inversion the valley-orbit and spin-orbit splittings of electron energy levels are strongly suppressed. This effect is quite unusual because typically a higher symmetry of a physical system implies a higher degeneracy of its energy levels, while in our case the suppression of the splittings occurs in NCs having lower symmetry. Nevertheless, we were able to explain this puzzling behavior using the mathematical apparatus of the group theory.

The confinement-induced intervalley splittings of electron levels can in principle be analyzed by either *ab initio* calculations[14,15] or semi-empirical atomistic methods.[6,7] The present-day first-principle calculations based on the density functional theory[14,15] do not yet allow for a comprehensive analysis of the intervalley splittings (see Refs. 16 and 17 for details). The semi-empirical methods, on the other hand, can handle NCs of any size and are versatile in terms of the involved physics. In this work we develop a semi-empirical $sp^3d^5s^*$ tight-binding (TB) method for lead chalcogenides.

II. TIGHT-BINDING PARAMETRIZATION

Lead chalcogenides (PbSe, PbS) are semiconductor compounds with a rocksalt crystal lattice and a narrow and direct bandgap.[18] The extrema of both the conduction and valence bands are located at the four L points of the Brillouin zone

$$\boldsymbol{k}_{1,2} = \frac{\pi}{a}(1,\pm1,\pm1), \quad \boldsymbol{k}_{3,4} = \frac{\pi}{a}(-1,\pm1,\mp1), \qquad (1)$$

where a is the lattice constant. The success of the empirical TB method depends on the choice of basis functions and on the accuracy of the fit of the bulk band structure. The simplest TB parametrizations of lead chalcogenides are based on the basis set of the three p orbitals playing a major role in the formation of the valence and conduction band states.[19,20] More quantitatively accurate models include also s^* and d orbitals.[6,21–23] However, no attempts (with the only exception of Ref. 20) have been made to fit the actual effective masses of the electrons and holes near the L points. On the other hand, the second-nearest neighbors p^3 model of Ref. 20 fails to reproduce the bulk dispersion for wave vectors far from the L points.[7] Consequently, even the most advanced existing TB parametrizations of lead chalcogenides[6] are not suitable[24] for an adequate description of the NCs.

We have performed an independent atomistic $sp^3d^5s^*$ TB parametrization of the electron energy dispersion in bulk PbSe and PbS by fitting the spectra calculated by the state-of-the art many-body technique of Ref. 16, known as GW approximation. The goal values for the carrier effective masses near the L points were set to the experimental values[25] $m_{c,l}^{\rm exp} = 0.070\,m_0$, $m_{c,t}^{\rm exp} = 0.040\,m_0$, $m_{h,l}^{\rm exp}$=$0.068\,m_0$, $m_{h,t}^{\rm exp}$=$0.034\,m_0$ for PbSe and $m_{c,l}^{\rm exp} = 0.105\,m_0$,$m_{c,t}^{\rm exp} = 0.080\,m_0$, $m_{h,l}^{\rm exp} = 0.105\,m_0$, $m_{h,t}^{\rm exp} = 0.075\,m_0$ for PbS (m_0 is the free electron mass), as even the modern *ab initio* approach[16] does not satisfactory reproduce the effective masses.

The TB parameters we obtained are listed in Table I. The resulting effective masses $m_{c,l} = 0.068\,m_0$, $m_{c,t} = 0.041\,m_0$, $m_{h,l} = 0.069\,m_0$, $m_{h,t} = 0.039\,m_0$ for PbSe and $m_{c,l} = 0.098\,m_0$, $m_{c,t} = 0.079\,m_0$, $m_{h,l} = 0.104\,m_0$, $m_{h,t} = 0.074\,m_0$ for PbS are quite close to the experimental values. The spin-orbit coupling constants of p orbitals at Pb, Se, and S

TABLE I. TB parameters for PbSe and PbS. The transfer integrals are measured in eV and given in the Slater-Koster notations (Ref. 26). The spin-orbit splittings are defined according to Ref. 27.

	PbS	PbSe		PbS	PbSe
a_0, Å	5.900	6.100	$s_a^* p_c\sigma$	2.606	2.258
E_{sa}	−10.596	−10.722	$s_c^* p_a\sigma$	2.177	1.731
E_{sc}	−5.444	−6.196	$s_a d_c\sigma$	−1.852	−1.917
E_{pa}	−1.797	−1.463	$s_c d_a\sigma$	−1.399	−1.256
E_{pc}	4.819	4.279	$s_a^* d_c\sigma$	0.040	0.146
E_{da}	7.468	7.984	$s_c^* d_a\sigma$	−0.792	−0.271
E_{dc}	20.900	26.114	$pp\sigma$	2.223	2.159
E_{s^*a}	17.878	15.117	$pp\pi$	−0.468	−0.463
E_{s^*c}	25.807	28.244	$p_a d_c\sigma$	−1.200	−1.272
$ss\sigma$	−0.567	−0.292	$p_c d_a\sigma$	−1.219	−1.332
$s^*s^*\sigma$	−2.478	−1.346	$p_a d_c\pi$	0.442	0.912
$s_c s_a^*\sigma$	−1.535	−0.654	$p_c d_a\pi$	0.983	0.966
$s_a s_c^*\sigma$	−0.693	−1.743	$dd\sigma$	0.778	0.244
$s_a p_c\sigma$	1.623	1.611	$dd\pi$	1.202	1.826
$s_c p_a\sigma$	1.371	1.291	$dd\delta$	−1.305	−1.235
Δ_a	0.096	0.420	Δ_c	2.380	2.380

were not changed during the fitting procedure and were taken from Refs. 28 and 29 for Pb and for the anions, respectively. Calculated dispersion, shown in Fig. 1 by the dotted curves, demonstrates a good overall agreement with the GW results (solid curves).

III. APPLICATION OF THE MODEL TO NANOCRYSTALS

When modeling lead salt NCs one should take into account that the actual structure of realistic quantum dots (QDs) depends on the specific growth procedure and may vary from sample to sample. Although the structure can be determined using nuclear magnetic resonance,[30] x-ray diffraction, and electron microscopy,[9,10,13] only few studies[11,30] went beyond a simple statement of a crystalline structure.

Among the samples studied to date, one can distinguish NCs belonging to one of the two types. The first type (I) is characterized by nonstoichiometry. NCs of this type were

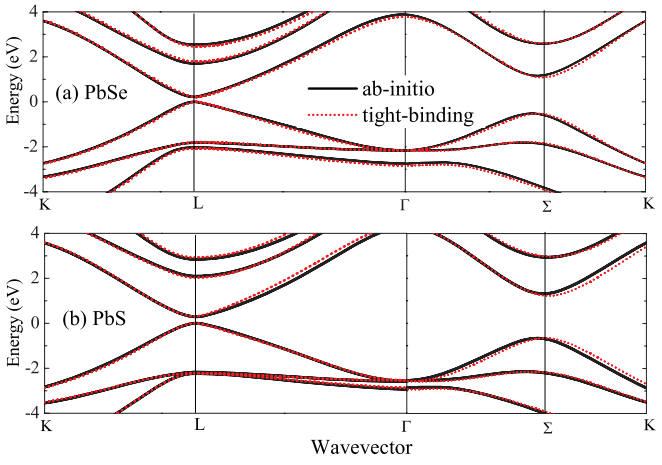

FIG. 1. (Color online) Electron energy dispersion of bulk (a) PbSe and (b) PbS calculated *ab initio* (Ref. 16) (solid line) and by the tight-binding method with the parameters of Table I (dashed line).

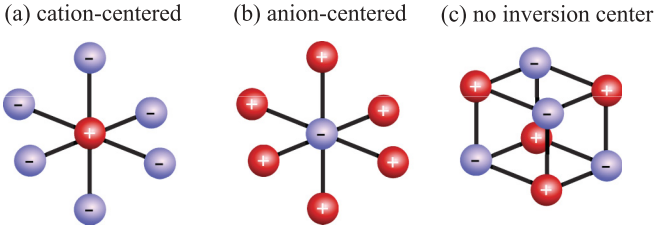

FIG. 2. (Color online) Central parts of the three types of nanocrystals.

studied by Moreels *et al.*[12] NCs of the second type (II) are characterized by the lack of a center of inversion. Samples of this type were reported by Cho *et al.*[11]

In our study we will consider NC geometries belonging to one of these two types. They are illustrated in Fig. 2. For the structures of types Ia and Ib, shown in Figs. 2(a) and 2(b), the center of the spherical NC is on a cation (anion) atom while for the structure in Fig. 2(c) the center of the sphere lies halfway between a cation and an anion on a line parallel to the [111] direction. The nonstoichiometric QDs of the types Ia and Ib both have centers of inversion and are characterized by the cube symmetry group O_h. The stoichiometric QD of the type II has no inversion center and is characterized by the tetrahedron symmetry group T_d. A theoretical study of such idealized structures with different symmetries is a prerequisite to understanding the fundamental physics of more realistic structures.

Note that the QDs in our model cannot be perfectly spherical due to the discreteness and lower point symmetry of the underlying crystal lattice. In our work the QDs are formed by all the atoms within a certain distance from the center of the NC. It is convenient to measure this distance with a dimensionless integer number. Thus, we define the "number of shells" as the number of atomic layers within the distance from the center of the QD to its surface along the [100] direction.

Usually one should consider the impact of surface passivation when calculating the confined states in a nanocrystal. Passivation of the dangling bonds is a characteristic feature of NCs made from covalent semiconductors, like Si (Ref. 31). In particular, the ground valence and conduction band states in Si are formed by bonding and antibonding orbitals, which are nonzero on both atoms of the unit cell. For nonpassivated surfaces this leads to the appearance of defect states lying inside the bandgap of Si NCs.[32] However, the situation is considerably different for lead chalcogenides,[31] which are characterized by strongly ionic atomic bonds making them relatively insensitive to the surface chemistry.[24] Due to the strong ionicity, the ground-state orbitals are strongly localized either on an anion or on a cation. As a result, no surface states appear in the fundamental bandgap of nonpassivated lead chalcogenide NCs, as has been also indicated by other TB studies.[6,24] Consequently, in our calculations we do not passivate surfaces, unless otherwise stated. In real QDs of the types Ia and Ib (cf. Fig. 2) such passivation might be necessary to compensate for the surface charge.[33]

Another important effect is the relaxation of the lattice in the nanocrystal from the ideal bulk rocksalt structure near the NC

surface. For PbSe NCs this effect was studied by Franceschetti using the density functional approach.[14] He found that Pb–Se bonds are significantly distorted within an approximately 8-Å-thick layer near the NC surface. However, his work totally neglected the spin-orbit coupling which is of key importance for our study and can be accurately accounted for in tight-binding calculations. To take into account lattice relaxation within the tight-binding model one has (i) to find optimized atomic positions minimizing the total energy of the system and (ii) to recalculate transfer integrals for the relaxed lattice. However, the almost ferroelectric nature of lead salts[34] presents a real challenge to the theorist. Even the calculation of phonon spectra in bulk lead salt compounds involves difficulties.[35] On the other hand, the analysis of the strain dependence of the transfer integrals of the tight-binding method in the case of lead salts is hindered by the lack of reliable band-structure calculations of strained lead salts.[36]

In any case, both surface passivation and surface relaxation are not as important for ionic materials as for covalent semiconductors. A simple termination of the bulk lattice structure is considered to be a satisfactory approximation for ionic materials[6,24,31] and we adhere to it here.

The calculated energy levels of confined carriers for PbSe and PbS NCs of the diameter $D \approx 5$ nm (corresponding to nine shells) are shown in Fig. 3. For each material three panels [Figs. 3(a)–3(c) and 3(a′)–3(c′)] correspond to the three possible NC geometries Ia, Ib, and II, illustrated in Fig. 2. The bandgap in both cases agrees well with the results of the authors of Ref. 6.

All the states can be divided into distinct groups characterized by a certain parity. For NCs with a center of inversion, each state automatically has a certain parity. Indeed, in bulk lead chalcogenides the lowest electron state in the conduction band has the L_6^- symmetry[16] (i.e., it is odd with respect to the inversion symmetry operation when the center of inversion is chosen on the cation atom). The uppermost electron state in the valence band has the opposite parity. For QDs without an inversion center one can define approximate projectors to the even and odd states. We have attributed a certain parity to the states, for which the squared projections differed more than in three times.

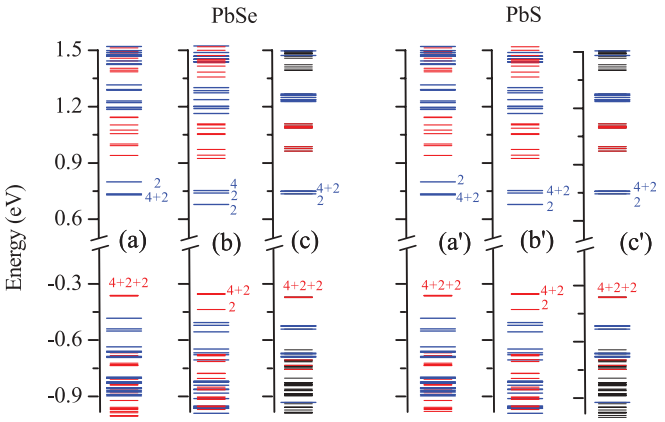

FIG. 3. (Color online) Energy levels in (a–c) PbSe and (a′, b′, c′) PbS NCs with diameter $D \approx 4.9$ and $D \approx 4.6$ nm, respectively. Panels (a–c) and (a′–c′) correspond to cation-centered NCs, anion-centered NCs and NCs without an inversion center, respectively (see Fig. 2). States of the odd and even parities are marked by the long, thick blue and short, thick red lines, respectively. The thin black lines correspond to the states without a certain parity. The degeneracies of the lowest electron and hole confined states are indicated near each line.

Energy splittings within each multiplet characterized by a certain parity are clearly seen in Fig. 3 and can be explained by the confinement-induced intervalley coupling and the carrier effective mass anisotropy. The importance of these two effects for lead chalcogenide NCs has been emphasized in Ref. 7. However, the dependence of the splittings on the NC geometry clearly manifested in Fig. 3 has never been reported.

A striking feature of Fig. 3(c) is the suppression of the energy splittings for the type II NCs lacking a center of inversion. The splittings are quite small and cannot be distinguished within the energy scale of Fig. 3. On the contrary, for QDs with an inversion center [Figs. 3(a), 3(b), 3(a′), and 3(b′)], the ground-state multiplets for both electrons and holes have well-pronounced structures with substantial splittings even for QD diameters as large as 4.9 nm. This observation refers to both the conduction and valence band electron states. The effect is more pronounced for the PbS QDs than for the PbSe QDs, which can be related to the more isotropic effective masses of the band extrema in bulk PbS.

To demonstrate the robustness of the splitting suppression in type II NCs we show in Fig. 4 energy levels calculated for small PbS NCs with diameter $D \sim 2.5$ nm. Levels in Figs. 4(a′)–4(c′) were calculated using the same boundary conditions as in Fig. 3, without passivation. Levels in Figs. 4(a)–4(c) were calculated for a NC with the same core, coated by an extra single-layer shell of atoms. For the shell layer the positive (negative) atomic energies of the orbitals were increased (decreased) by 4 eV, respectively. As a result, the NC boundary potential effectively becomes more smooth than in a NC without coating. Comparing Figs. 4(a)–4(c) and 4(a′)–4(c′) we see that the bandgap of a NC is slightly affected by the coating. On the other hand, the valley splittings are very sensitive to the properties of the boundary and are substantially quenched for the coated NCs having a smoother boundary. Nevertheless, the splittings are substantially suppressed in coated type II NCs

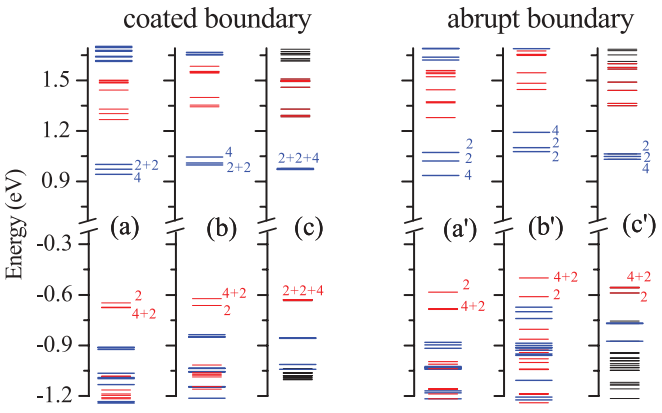

FIG. 4. (Color online) Energy levels in PbS NCs with core diameter $D \approx 2.5$ nm with (a–c) coated and (a′–c′) abrupt boundary. Notation is the same as on Fig. 4. Calculation details are given in the text.

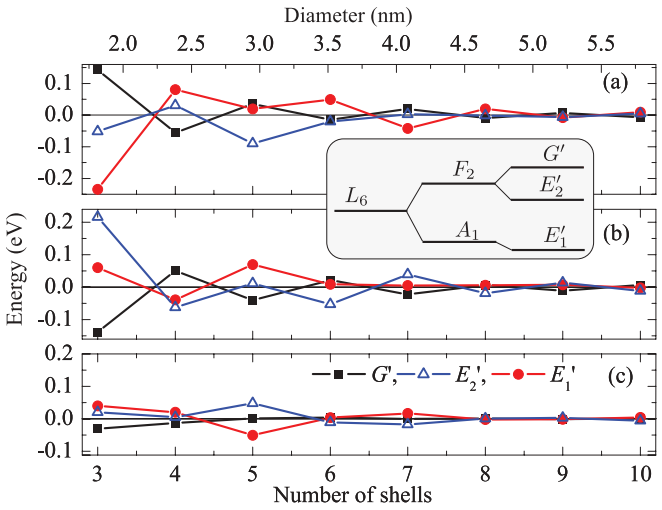

FIG. 5. (Color online) Energies of levels belonging to the ground state multiplet of the conduction band electron in PbS NCs as functions of NC diameter. Panels (a), (b), and (c) correspond to Pb-centered NCs, S-centered NCs, and NCs without inversion center, see Fig. 2. Squares, triangles, and circles correspond to the states with the symmetry G', E_2', and E_1', respectively, see the level splitting scheme in the inset.

as compared to those of type I, see Fig. 4(c). This is a strong signature of a physical effect, demanding an explanation.

To analyze this puzzling behavior more systematically, we have studied the dependence of the splittings on the NC diameter. For simplicity, we restrict our consideration by the electron and hole ground states. Within the effective mass approximation, the ground state of confined carriers is fourfold degenerate with respect to the valley index and twofold degenerate with respect to the spin projection (i.e., the total degeneracy is eightfold). If we neglect the spin and consider the valley-orbit interaction only, the ground state is split into a state of A_1 symmetry (singlet) and a state of F_2 symmetry (triplet), as sketched in the insets of Figs. 5 and 6. When the spin degree of freedom is taken into account then both the singlet and the triplet states acquire extra degeneracy.

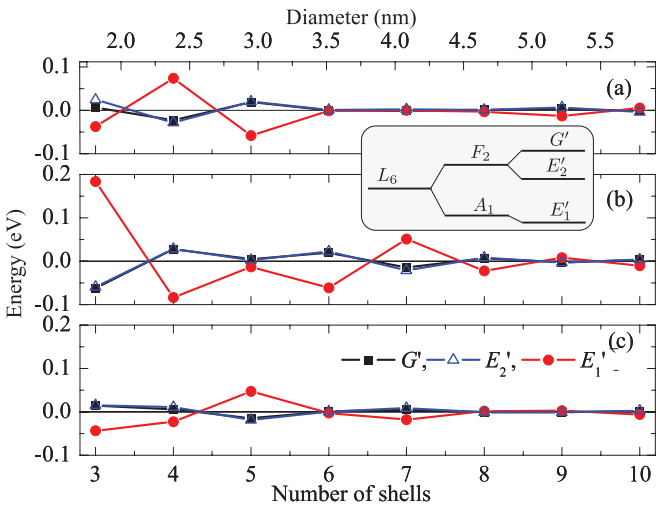

FIG. 6. (Color online) Same as Fig. 5, but for the valence-band ground state.

This degeneracy is partly lifted, as the sixfold degenerate state corresponding to the triplet is split by the spin-orbit interaction into a twofold degenerate state of E_2' symmetry and a fourfold degenerate state of G' symmetry.[37] As a result, the carrier ground-state level is split into the three multiplets: the two doublets (of E_1' and E_2' symmetry, respectively) and the fourfold degenerate state of G' symmetry. As far as the spatial inversion is not considered, the symmetry groups T_d and O_h are equivalent. Therefore, this symmetry analysis applies to all types of NC geometries presented in Fig. 2.

Figures 5 and 6 show the energies of the resulting conduction (valence) band multiplets in PbS NCs as functions of the NC diameter. Figures 5(a)–5(c) and 6(a)–6(c) correspond to the three NC geometries considered throughout the paper (see Fig. 2). The energies of the states are counted from the averaged value $(E_{E_1'} + E_{E_2'} + 2E_{G'})/4$. The splittings strongly oscillate with the number of shells N in a NC. Such oscillations are typical for the valley splittings in various semiconductor structures. Similar behavior has been reported for SiGe/Si (Refs. 38 and 39) and GaSb/AlAs (Refs. 40 and 41) quantum wells and Si NCs.[42] The phase of the oscillations is determined by the product of the intervalley wave vector and the structure size.

A comparison of Figs. 5(a), 5(b), 6(a), and 6(b) on one hand with Figs. 5(c) and 6(c), on the other hand, clearly shows that the suppression of valley splittings in NCs without a center of inversion is a general feature persistent in a wide range of NC sizes. The vertical scale on all the panels of Figs. 5 and 6 is the same and the overall span of the points on Figs. 5(c) and 6(c) is substantially smaller. Although certain exceptions from this rule are possible, for example, for the valence-band state with five shells, see Fig. 6, the suppression of splittings is quite systematic.

A comparison of Figs. 5 with 6 also enables one to conclude that the spin-orbit interaction is much stronger for conduction-band electrons than for valence-band holes. Indeed, the energies of the hole states with the symmetry G' and E_2' in Fig. 6 are almost the same, while, for conduction-band electrons, all the splittings in Fig. 5 are of the same order.

IV. SYMMETRY ANALYSIS

Let us explain the anomalous suppression of the valley splittings in lead salt NCs without an inversion center. We want to account for the intervalley coupling in the lowest nonvanishing approximation. To this end, we consider electronic states originating from the four inequivalent L valleys of a bulk semiconductor and neglect the $\boldsymbol{k}\cdot\mathbf{p}$ mixing of conduction and valence band states.[18] Then the wave function of the confined electron state in the jth L valley can be written as $\langle \boldsymbol{r}|L_j\rangle = e^{i\boldsymbol{k}_j\boldsymbol{r}}u_j(\boldsymbol{r})\Phi_j(\boldsymbol{r})$, where $\Phi_j(\boldsymbol{r})$ is the smooth envelope function, $u_j(\boldsymbol{r})$ is the periodic Bloch amplitude for the bulk state in the jth valley, and spin indices are omitted. We will further assume that the bulk material has the isotropic effective masses of the band extrema in L points. In this approximation the envelopes $\Phi_j(\boldsymbol{r})$ are invariant under rotations. The confinement-induced intervalley coupling can be described by the following matrix element:

$$I_{j,k} = \langle L_j|H_{\mathrm{QD}}|L_k\rangle, \quad j,k = 1\ldots4, \quad j \neq k, \qquad (2)$$

TABLE II. Phase factors in Eq. (3) for the coordinates of the anion atoms in Fig. 2(c).

	$\frac{a}{4}(1,1,1)$	$\frac{a}{4}(1,\bar{1},\bar{1})$	$\frac{a}{4}(\bar{1},1,\bar{1})$	$\frac{a}{4}(\bar{1},\bar{1},1)$	
$e^{i(\boldsymbol{k}_1-\boldsymbol{k}_2)\boldsymbol{R}_n}$	-1	-1	1	1	$-x$
$e^{i(\boldsymbol{k}_1-\boldsymbol{k}_3)\boldsymbol{R}_n}$	-1	1	-1	1	$-y$
$e^{i(\boldsymbol{k}_1-\boldsymbol{k}_4)\boldsymbol{R}_n}$	-1	1	1	-1	$-z$

where H_{QD} is the microscopic QD Hamiltonian. Then it follows that the integral $I_{j,k}$ vanishes when the QD lacks inversion symmetry (i.e. belongs to the type II). To show this let us rewrite $I_{j,k}$ as

$$I_{j,k} \approx \int_{\mathrm{u.c.}} e^{-i\boldsymbol{k}_j\boldsymbol{r}}\, u_j^*(\boldsymbol{r}+\boldsymbol{\tau})\, H_{\mathrm{bulk}}\, e^{i\boldsymbol{k}_k\boldsymbol{r}}\, u_k(\boldsymbol{r}+\boldsymbol{\tau}) d\boldsymbol{r} \times \sum_{\mathbf{R}_n} e^{i(\boldsymbol{k}_k-\boldsymbol{k}_j)\boldsymbol{R}_n}\, \Phi_j^*(\boldsymbol{R}_n)\, \Phi_k(\boldsymbol{R}_n)\,, \tag{3}$$

where the integral in the right-hand side is over a unit cell and contains the Hamiltonian of a bulk material, $\boldsymbol{\tau}$ determines the position of a cation (or anion) atom with respect to the center of the unit cell, and the summation runs over all the cation (or anion) sites *within the QD*. It is this summation that is sensitive to the arrangement of atoms within the QD. For the type II geometry the sum is exactly zero. This cancellation takes place independently of the radius of the QD and is fully determined by the symmetry. To see this one can use the following well-known fact.[37] If a given function describing some crystalline physical system transforms according to a certain representation of the system's symmetry group, then the sum of this function over the lattice sites belonging to the system may be different from zero if and only if the decomposition of this representation into irreducible ones contains the identity representation.

In our case one can distinguish three linearly independent functions $\exp[i(\boldsymbol{k}_k-\boldsymbol{k}_j)\boldsymbol{R}_n]$ which may be chosen as shown in the first column of Table II. Table II gives the values of these exponent functions when $\boldsymbol{R}_n$ sweeps the coordinates of the anion atoms shown in Fig. 2(c). These atoms may be obtained from one another by the rotations of the type II QD. The last column of Table II indicates that the exponent functions transform according to the vector irreducible representation F_2 of the group T_d. This representation is different from the identity representation A_1. Therefore, for type II QDs Eq. (3) is zero. Table III gives the values of the same exponent functions when $\boldsymbol{R}_n$ sweeps the coordinates of the anion atoms shown in Fig. 2(a). These atoms may be obtained from one another by the rotations of the type Ia QD. The last row of Table III shows that the sum of the exponent functions remains invariant under such rotations. More precisely, the exponent functions transform according to the direct sum of the two irreducible

TABLE III. Same as Table II but for anion atoms in Fig. 2(a).

	$(\pm\frac{a}{2},0,0)$	$(0,\pm\frac{a}{2},0)$	$(0,0,\pm\frac{a}{2})$	
$e^{i(\boldsymbol{k}_1-\boldsymbol{k}_2)\boldsymbol{R}_n}$	1	-1	-1	
$e^{i(\boldsymbol{k}_1-\boldsymbol{k}_3)\boldsymbol{R}_n}$	-1	1	-1	
$e^{i(\boldsymbol{k}_1-\boldsymbol{k}_4)\boldsymbol{R}_n}$	-1	-1	1	
$\sum_{j=2}^{4} e^{i(\boldsymbol{k}_1-\boldsymbol{k}_j)\boldsymbol{R}_n}$	-1	-1	-1	A_1^+

representations $A_1^+ \oplus E^+$ of the group O_h. Thus, for type Ia QDs Eq. (3) is different from zero.

This consideration is no longer valid if the function $\Phi_j(\boldsymbol{r})$ is anisotropic. This is the case of real lead salt NCs, as in bulk lead chalcogenides the longitudinal mass in the L valley is larger than the transverse one. Consequently, in real NCs lacking an inversion center the valley splitting is not exactly zero but determined by the degree of the effective mass anisotropy in L valleys. This explains the fact that in PbS NCs the splitting is smaller than in PbSe ones [cf. Figs. 3(c) and 3(c′)]. The nonzero valley splittings in lead salt NCs without a center of inversion may also result from the $\boldsymbol{k}\cdot\boldsymbol{p}$-induced mixing of the conduction and valence band states[18] or from an admixture of the states originating from other band extrema of a bulk semiconductor to the wave functions of the electron and hole ground states.[7] For certain small sizes the latter effect may be efficient and can explain the absence of splitting suppression for hole states in a five-shell NC, see Fig. 6(c).

V. CONCLUSION

In conclusion, we obtained a new set of $sp^3d^5s^*$ TB parameters for the bulk PbSe and PbS semiconductor compounds and calculated the electron and hole energy levels in NCs made of these materials. We demonstrated that the valley-orbit and spin-orbit splittings of the ground state of electrons and holes are very sensitive to a particular arrangement of atoms in the NC and can be strongly suppressed for a certain geometry, when the NC lacks a center of inversion.

ACKNOWLEDGMENTS

Useful discussions with E. L. Ivchenko and L. E. Golub are gratefully acknowledged. This work was supported by the Russian Foundation for Basic Research, European projects POLAPHEN and Spin-Optronics, and the "Dynasty" Foundation-ICFPM. The work of S.V.G. was supported, in part, by the Research Corporation for Science Advancement under Award No. 20081 and, in part, by the National Science Foundation under Grant No. HRD-0833178. The work of M.O.N. was partially supported by "Triangle de la Physique."

[1] R. J. Ellingson, M. C. Beard, J. C. Johnson, P. Yu, O. I. Micic, A. J. Nozik, A. Shabaev, and A. L. Efros, Nano Lett. **5**, 865 (2005).
[2] R. D. Schaller and V. I. Klimov, Phys. Rev. Lett. **92**, 186601 (2004).
[3] M. T. Trinh, A. J. Houtepen, J. M. Schins, T. Hanrath, J. Piris, W. Knulst, A. P. L. M. Goossens, and L. D. A. Siebbeles, Nano Lett. **8**, 1713 (2008).
[4] M. C. Beard, A. G. Midgett, M. Law, O. E. Semonin, R. J. Ellingson, and A. J. Nozik, Nano Lett. **9**, 836 (2009).
[5] O. E. Semonin, J. M. Luther, S. Choi, H.-Y. Chen, J. Gao, A. J. Nozik, and M. C. Beard, Science **334**, 1530 (2011).
[6] G. Allan and C. Delerue, Phys. Rev. B **70**, 245321 (2004).

[7]J. M. An, A. Franceschetti, S. V. Dudiy, and A. Zunger, Nano Lett. **6**, 2728 (2006).
[8]A. Rogach, A. Eychmüller, S. Hickey, and S. Kershaw, Small **3**, 536 (2007).
[9]W. W. Yu, J. C. Falkner, B. S. Shih, and V. L. Colvin, Chem. Mater. **16**, 3318 (2004).
[10]H. Du, C. Chen, R. Krishnan, T. D. Krauss, J. M. Harbold, F. W. Wise, M. G. Thomas, and J. Silcox, Nano Lett. **2**, 1321 (2002).
[11]K.-S. Cho, D. V. Talapin, W. Gaschler, and C. B. Murray, J. Am. Chem. Soc. **127**, 7140 (2005).
[12]I. Moreels, K. Lambert, D. De Muynck, F. Vanhaecke, D. Poelman, J. C. Martins, G. Allan, and Z. Hens, Chem. Mater. **19**, 6101 (2007).
[13]V. Petkov, I. Moreels, Z. Hens, and Y. Ren, Phys. Rev. B **81**, 241304 (2010).
[14]A. Franceschetti, Phys. Rev. B **78**, 075418 (2008).
[15]Y. Gai, H. Peng, and J. Li, J. Phys. Chem. C **113**, 21506 (2009).
[16]A. Svane, N. E. Christensen, M. Cardona, A. N. Chantis, M. van Schilfgaarde, and T. Kotani, Phys. Rev. B **81**, 245120 (2010).
[17]A. Łusakowski, P. Bogusławski, and T. Radzyński, Phys. Rev. B **83**, 115206 (2011).
[18]I. Kang and F. W. Wise, J. Opt. Soc. Am. B **14**, 1632 (1997).
[19]D. L. Mitchell and R. F. Wallis, Phys. Rev. **151**, 581 (1966).
[20]B. Volkov, O. Pankratov, and A. Sazonov, Soviet J. Experimental Theoretical Phys. **58**, 809 (1983).
[21]C. S. Lent, M. A. Bowen, J. D. Dow, R. S. Allgaier, O. F. Sankey, and E. S. Ho, Superlattices Microstruct. **2**, 491 (1986).
[22]M. Lach-hab, D. A. Papaconstantopoulos, and M. J. Mehl, J. Phys. Chem. Solids **63**, 833 (2002).
[23]J. A. Valdivia and G. E. Barberis, J. Phys. Chem. Solids **56**, 1141 (1995).
[24]A. Paul and G. Klimeck, Appl. Phys. Lett. **98**, 212105 (2011).
[25]H. Preier, Appl. Phys. A **20**, 189 (1979).
[26]J. C. Slater and G. F. Koster, Phys. Rev. **94**, 1498 (1954).
[27]D. J. Chadi, Phys. Rev. B **16**, 790 (1977).
[28]F. Herman, C. D. Kuglin, K. F. Cuff, and R. L. Kortum, Phys. Rev. Lett. **11**, 541 (1963).
[29]F. Herman and S. Skillman, *Atomic Structure Calculations* (Prentice-Hall, Englewood Cliffs, NJ, 1963).
[30]I. Moreels, B. Fritzinger, J. C. Martins, and Z. Hens, J. Am. Chem. Soc. **130**, 15081 (2008).
[31]W. Harrison, *Elementary Electronic Structure* (World Scientific, Singapore, 2004).
[32]C. Delerue and M. Lannoo, *Nanostructures. Theory and Modelling* (Springer-Verlag, Berlin, 2004).
[33]R. Leitsmann and F. Bechstedt, ACS Nano **3**, 3505 (2009).
[34]H. Bilz, A. Bussmann-Holder, W. Jantsch, P. Vogl, A. Bussmann-Holder, H. Bilz, and R. Vogl, in *Dynamical Properties of IV-VI Compounds*, Vol. 99 of *Springer Tracts in Modern Physics*, (Springer, Berlin, 1983), pp. 51–98.
[35]O. Kilian, G. Allan, and L. Wirtz, Phys. Rev. B **80**, 245208 (2009).
[36]N. E. Christensen, A. Svane, M. Cardona, A. N. Chantis, R. Laskowski, M. van Schilfgaarde, and T. Kotani, Phys. Status Solidi B **248**, 1096 (2011).
[37]G. Bir and G. Pikus, *Symmetry and Strain-Induced Effects in Semiconductors* (Wiley, New York, 1974).
[38]M. O. Nestoklon, L. E. Golub, and E. L. Ivchenko, Phys. Rev. B **73**, 235334 (2006).
[39]M. Friesen, S. Chutia, C. Tahan, and S. N. Coppersmith, Phys. Rev. B **75**, 115318 (2007).
[40]D. Z.-Y. Ting and Y.-C. Chang, Phys. Rev. B **38**, 3414 (1988).
[41]J.-M. Jancu, R. Scholz, G. C. La Rocca, E. A. de Andrada e Silva, and P. Voisin, Phys. Rev. B **70**, 121306 (2004).
[42]C. Bulutay, Phys. Rev. B **76**, 205321 (2007).